SCIENTIFIC REPORTS
nature research

Check for updates

OPEN

Non-Mendelian inheritance during inbreeding of $Ca_v3.2$ and $Ca_v2.3$ deficient mice

Serdar Alpdogan[1,2], Renate Clemens[1,2], Jürgen Hescheler[1], Felix Neumaier[1] & Toni Schneider[1]✉

The mating of 77 heterozygous pairs ($Ca_v3.2$[+|−] x $Ca_v3.2$[+|−]) revealed a significant deviation of genotype distribution from Mendelian inheritance in weaned pups. The mating of 14 pairs ($Ca_v3.2$[−|−] female x $Ca_v3.2$[+|−] male) and 8 pairs ($Ca_v3.2$[+|−] female x $Ca_v3.2$[−|−] male) confirmed the significant reduction of deficient homozygous $Ca_v3.2$[−|−] pups, leading to the conclusion that prenatal lethality may occur, when one or both alleles, encoding the $Ca_v3.2$T-type Ca^{2+} channel, are missing. Also, the mating of 63 heterozygous pairs ($Ca_v2.3$[+|−] x $Ca_v2.3$[+|−]) revealed a significant deviation of genotype distribution from Mendelian inheritance in weaned pups, but only for heterozygous male mice, leading to the conclusion that compensation may only occur for $Ca_v2.3$[−|−] male mice lacking both alleles of the R-type Ca^{2+} channel. During the mating of heterozygous parents, the number of female mice within the weaned population does not deviate from the expected Mendelian inheritance. During prenatal development, both, T- and R-type Ca^{2+} currents are higher expressed in some tissues than postnatally. It will be discussed that the function of voltage-gated Ca^{2+} channels during prenatal development must be investigated in more detail, not least to understand devastative diseases like developmental epileptic encephalopathies (DEE).

Calcium ions are crucial for reproduction and development[1]. Changes of cytosolic Ca^{2+} concentrations translate a diverse set of signals into specific cellular responses. More than 100 Ca^{2+} channels, pumps, exchangers, sensors and buffers contribute to the fundamental processes involved in development and propagation of living cells[2]. Voltage-gated Ca^{2+} channels (VGCCs) are a key mediator of Ca^{2+} entry from the extracellular space and enable Ca^{2+} signaling in a dual manner, electrogenically, via Ca^{2+}-induced changes in membrane potential, and biochemically, through the activation of Ca^{2+} dependent enzymes and other proteins affecting cellular regulation[3].

Ten mammalian genes are known to encode different ion conducting $Ca_v\alpha1$ subunits of these VGCCs, which have been subdivided into 7 high- and 3 low-voltage activated Ca^{2+} channels (for details,[4]). In vivo, they are assembled with additional auxiliary subunits[5], for which the complete setup of components is only partially known. Additional structural variation arises from alternative splicing, which increases structural and functional variability[6,7].

The ion conducting $Ca_v\alpha1$ subunits of VGCCs have been inactivated in mice to deduce their individual functions[8]. Some of the resulting mouse models are related to human diseases (for a summary see:[9]).

Several voltage-gated Ca^{2+} channels play a role in rodent models of acquired epilepsy, including the $Ca_v2.3$ / R-type[10,11] and the $Ca_v3.2$/T-type channel[12,13], both of which are highly sensitive towards divalent trace metal cations[14,15,16]. Mouse models lacking both Ca^{2+} channel types were investigated in previous studies to describe in detail their phenotypes and sensitivities towards divalent metal cations when co-injected with kainate. During the breeding of these mice the number of weaned pups did not correspond the expected ratios for a Mendelian inheritance, pointing to a possible prenatal lethality.

[1]Institute for Neurophysiology, University of Cologne, Robert-Koch-Str. 39, 50931 Cologne, Germany. [2]These authors contributed equally: Serdar Alpdogan and Renate Clemens. ✉email: toni.schneider@uni-koeln.de

Material and methods

Material and reagents. Unless noted otherwise, all reagents were obtained from Sigma-Aldrich and used without further purification (Sigma-Aldrich Chemie GmbH, Schnelldorf, Germany). Solutions were prepared with deionized, double-distilled or type I ultrapure water dispensed from an ELGA LabWater (Purelab Flex 2, United Kingdom) system respectively.

Animals. Mice were housed at a constant temperature (20–22 °C) in makrolon type II cages, with light on from 7 a.m. to 7 p.m. (light intensity at the surface of the animal cages was between 5 and 10 lx) and ad libitum access to food and water.

The cacna1h gene encoding $Ca_v3.2$ was disrupted in mice by homologous recombination[17]. These mice were inbred in C57Bl/6 background for more than 10 generations. C57Bl/6J were used as $Ca_v3.2$-competent control mice. The strain abbreviation for the mouse line is C57Bl/6J-cacna1h$^{+|-}$ for the mice lacking one $Ca_v3.2$-allele (heterozygous mice) and C57Bl/6J-cacna1h$^{-|-}$ for the mice lacking both $Ca_v3.2$-alleles (homozygous mice deficient of $Ca_v3.2$). $Ca_v3.2$-deficient mice are available from Mutant Mouse Resource & Research Centers (MMRRC) with the strain name B6.129-Cacna1h^{tm1Kcam}/Mmmh.

The cacna1e gene encoding $Ca_v2.3$ was disrupted in vivo by agouti-colored $Ca_v2.3$(fl|+) and deleter mice expressing Cre-recombinase constitutively[18]. Thus, exon 2 was deleted by Cre-mediated recombination. $Ca_v2.3$-deficient mice were fertile, exhibited no obvious behavioral abnormalities and the born $Ca_v2.3$-deficient mice had the same lifespan as control mice. Parallel breeding of parental inbred mouse lines of $Ca_v2.3$-deficient and control mice ensured their identical background. The strain abbreviation for the mouse line is C57Bl/6.129SvJ-cacna1e$^{+|-}$ for the mice lacking one $Ca_v2.3$-allele (heterozygous mice) and C57Bl/6J-cacna1e$^{-|-}$ for the mice lacking both $Ca_v2.3$-alleles (homozygous mice deficient of $Ca_v2.3$). $Ca_v2.3$-deficient mice are available from MMRRC with the strain name B6J.129P2(Cg)-Cacna1e$^{tm1.1Tsch}$/Mmjax.

The animal experimentation described in the text was approved by the institutional committee on animal care (Landesamt für Natur, Umwelt und Verbraucherschutz North Rhine Westfalia, Az number 84-02.04.2013.A186 and 81-02.04.2018.A176) and conducted in accordance with accepted standards of humane animal care, as described in the UFAW handbook on the care and management of laboratory animals.

Genotyping of mice. Tail biopsies from 21 day old mice were used for the extraction of genomic DNA. Contaminating protein and RNA were enzymatically digested by protease and RNAse, respectively.

For the PCR amplification of indicative $Ca_v3.2$ DNA-fragments, about 1 µg DNA was introduced and amplified with the WT-forward primer 5′- ATT CAA GGG CTT CCA CAG GGT A-3′ and the WT-reverse / KO-forward primers 5′-CAT CTC AGG GCC TCT GGA CCA C-3′ and KO-reverse primer 5′-GCT AAA GCG CAT GCT CCA GAC TG-3′[17]. The sizes of DNA fragments expected are 480 bp for the WT and 330 for the $Ca_v3.2$-KOs.

For the PCR amplification of indicative $Ca_v2.3$ DNA-fragments, about 1 µg DNA was introduced and amplified with the forward primer (B45Hilx1) 5′-AAA AAC AGC CGG GGA AAG CTT AT-3′ and the reverse primer (a1eb45r) 5′-CTG CCC TTT CTT CTT GCC TGA C-3′. The sizes of DNA fragments expected are 1047 bp for the WT and 86 bp for the $Ca_v2.3$-KOs.

PCRs for both genotypings were performed using a DNAEngine Peltier thermal cycler (BioRad, Germany) or a PTC-200 Peltier thermal cycler (MJ Research, Biozym Diagnostik, Germany) with the initial denaturation (94 °C for 10 min) followed by 34 cycles (denaturation at 94 °C for 60 s, annealing at 60 °C for 90 s, extension at 72 °C 4 min) and final extension at 72 °C for 10 min. The PCR products were separated by agarose gel electrophoresis and fluorescent bands were detected on a Herolab UVT-28 M transilluminator by UV irradiation (312 nm excitation wavelength) (Fig. 1).

Data analysis and statistics. The assumption of normal distribution of data was tested by the Kolmogorov–Smirnov test. The Student's *t*-test was used for the comparison of two experimental groups. Data were analyzed by one-way ANOVA for multiple comparisons. Statistical analysis was performed with the GraphPad Prism software (version 8). The Mendelian genotype distributions were tested by a chi-square test for Mendelian ratios by the use of the algorithm on the web page https://www.ihh.kvl.dk/htm/kc/popgen/genetik/applets/ki.htm. The calculated chi-square values were evaluated and converted into a probability (p-)value by using tables 4-1[19].

Ethical approval. All applicable international, national and institutional guidelines for the care and use of animals were followed.

Results

During the routine breeding for $Ca_v3.2$-deficient mice over a time period of 12 years, the number of genotyped knockout mice (Fig. 1) was severely under represented (the distribution for the genotypes within each group of born mice is summarized in Supplement-table S1 to S3). The consecutive systematic evaluation of wild type, heterozygous and $Ca_v3.2$-deficient pups from 99 breeding pairs (Table 1) revealed a highly significant reduction of heterozygous and even more significant reduction of homozygous $Ca_v3.2$-deficient mice. For comparison, the breeding history was also analyzed for the $Ca_v2.3$-deficient mouse lines.

Analysis of the genotypes for $Ca_v3.2$/T-type mice. $Ca_v3.2$ channels mediating T-type Ca^{2+} currents have been inactivated in mice by homologous recombination[17]. The deletion of exon 6 of the murine cacna1h

Genotype of parents		Statistics of pups and genotype distribution					
Female(s)	Male	Mating pairs (n)	Mean litter size Female pups	Genotype deviation Chi-squared p	Mean litter size Male pups	Genotype deviation Chi-squared p	Sex ratioF / M
$Ca_v3.2(+\|-)$	$Ca_v3.2(+\|-)$	77	2.95 ± 0.25	< 0.01	2.97 ± 0.22	< 0.001	1.28 ± 0.17
$Ca_v3.2(-\|-)$ $Ca_v3.2(+\|-)$	$Ca_v3.2(+\|-)$ $Ca_v3.2(-\|-)$	14 8	1.68 ± 0.22	> 0.05	2.41 ± 0.33	<0.01	0.71 ± 0.13 (p = 0.07 *)
$Ca_v2.3(+\|-)$	$Ca_v2.3(-\|-)$	63	3.29 ± 0.21	>0.1	3.59 ± 0.21	< 0.005	1.05 ± 0.07

Table 1. Litter sizes for male and female weaned pups and deviations of genotype distribution from Mendelian inheritance. Mating pairs with a homozygous $Ca_v3.2(-|-)$ partner are summarized because of the low number of events (line in the middle of the table). * = For the summarized data in this table line, no significant difference was observed. However, in 8 matings with a homozygous male and a heterozygous female partner the number of female pups was significantly reduced (p = 0.023, Students t-test).

gene was designed to delete the IS5 region in the channel protein and to impair the synthesis of a functional full-length protein. It caused a severe reduction of $Ca_v3.2$ mRNA in heterozygous mice as quantified by Northern blot analysis and a complete loss of $Ca_v3.2$ mRNA in $Ca_v3.2$-deficient mice. In differentiated myotubes from the individual genotypes, the transcript for $Ca_v3.2$ identified by RT-PCR was well detected in $Ca_v3.2$-competent and completely lost in $Ca_v3.2$-deficient mice. Simultaneously, the amount of transcript for $Ca_v3.1$ was strongly increased in these myotubes[17], suggesting a compensatory upregulation of these channels.

PCR-genotyping results. The genotyping of the litter was performed postnatally by PCR on total DNA isolated from tail biopsies (Fig. 1C,D). The amplified DNA fragments were clearly separated from each other by agarose gel electrophoresis to ensure exact genotype identification (Fig. 1A). The oligonucleotide primers were designed to detect easily and precisely DNA fragments from wild type and $Ca_v3.2$ deficient mice. The intensities of DNA fragments were strong enough to identify wild type (3 mice plus 1 reference DNA), heterozygous (11 mice plus 1 reference DNA) and $Ca_v3.2$-deficient candidates (3 candidates plus 1 reference DNA) (Fig. 1A). The negative control (no tail DNA included) did not contain DNA fragments of the references sizes (480 bp for wt or 330 bp for KO).

Distribution of individual genotypes in the mouse lines for the $Ca_v3.2$ gene inactivation. During 77 breeding events from heterozygous parents, in total 83 male $Ca_v3.2(+|+)$ mice were born (Suppl.-Tab. 1). As null hypothesis and according to Gregor Mendel[20], one would expect 166 heterozygous and 83 homozygous male $Ca_v3.2$-deficient pups, following the law of independent assortment. But during the investigated years of breeding only 111 heterozygous and 35 $Ca_v3.2$-deficient pups were born (Suppl.-Tab. 1). Similar results were achieved for the females. During the same 77 breedings, in total 72 $Ca_v3.2(+|+)$ female mice were born. Again, as null hypothesis with Mendelian inheritance, one would expect 144 heterozygous and 72 homozygous female $Ca_v3.2$-deficient pups. However, only 116 heterozygous and 39 $Ca_v3.2$-deficient pups were weaned (Suppl.-Tab. 1). Consecutively, the observed genotype distribution differed from the expected Mendelian ratio and the deviation was significant as deduced from the Chi-squared derived (CHSQ) p-values for both, males ($p < 0.001$) and females ($p < 0.01$) (Table 1).

For another statistical comparison, the mean values of pups per breeding for each sex and genotype were calculated (Fig. 2A). Heterozygous mice from both sexes were still superior in number (1.3-fold for males and 1.6-fold for females), but did not reach the two-fold majority predicted from theory. When comparing the expected two-fold number with the real number of heterozygous pups, it was significantly reduced for both sexes (p = 0.0002 for males and p = 0.0023 for females) (see red stars in Fig. 2A).

When comparing the homozygous $Ca_v3.2$-deficient mice from both sexes with the homozygous $Ca_v3.2$-competent mice, they were significantly reduced as well ($p < 0.001$ for males and p = 0.009 for females) (Fig. 2A).

During 22 breeding events, one parent was heterozygote and the other homozygote. According to Gregor Mendel, half of the pups should be heterozygotes and the other half homozygote for $Ca_v3.2$-deficiency. However, in both sexes, the number of $Ca_v3.2$ deficient mice was reduced. While 36 heterozygous male pups were born, only 17 homozygous Cav3.2 null mice were born (for females 24 heterozygous pups and only 13 null mice). Thus, the ratio was significant reduced for the male $Ca_v3.2$-deficient mice (p = 0.007 for males and p = 0.063 for females) (Fig. 2B), leading to the conclusion that the null hypothesis has to be rejected and that as an alternative hypothesis, the inactivation of the $Ca_v3.2$ gene in mice may cause prenatal lethality, which does not penetrate to all but to many of the individuals.

Analysis of the genotypes for $Ca_v2.3$/R-type mice. Next, we were interested in the breeding results for $Ca_v2.3$-deficient mice, which are known to exhibit a deficit in the flagellar speed of moving sperms as well as in the acrosome reaction[21,22]. The $Ca_v2.3$ channels mediating R-type Ca^{2+} currents have been inactivated in mice by homologous recombination and by successive breeding with cre-deleter mice[23]. The deletion of exon 2 of the murine cacna1e gene was designed to delete the IS1 region in the channel protein and to impair the synthesis of a functional full length channel transcript. It caused the complete loss of $Ca_v2.3$ channel protein as proven

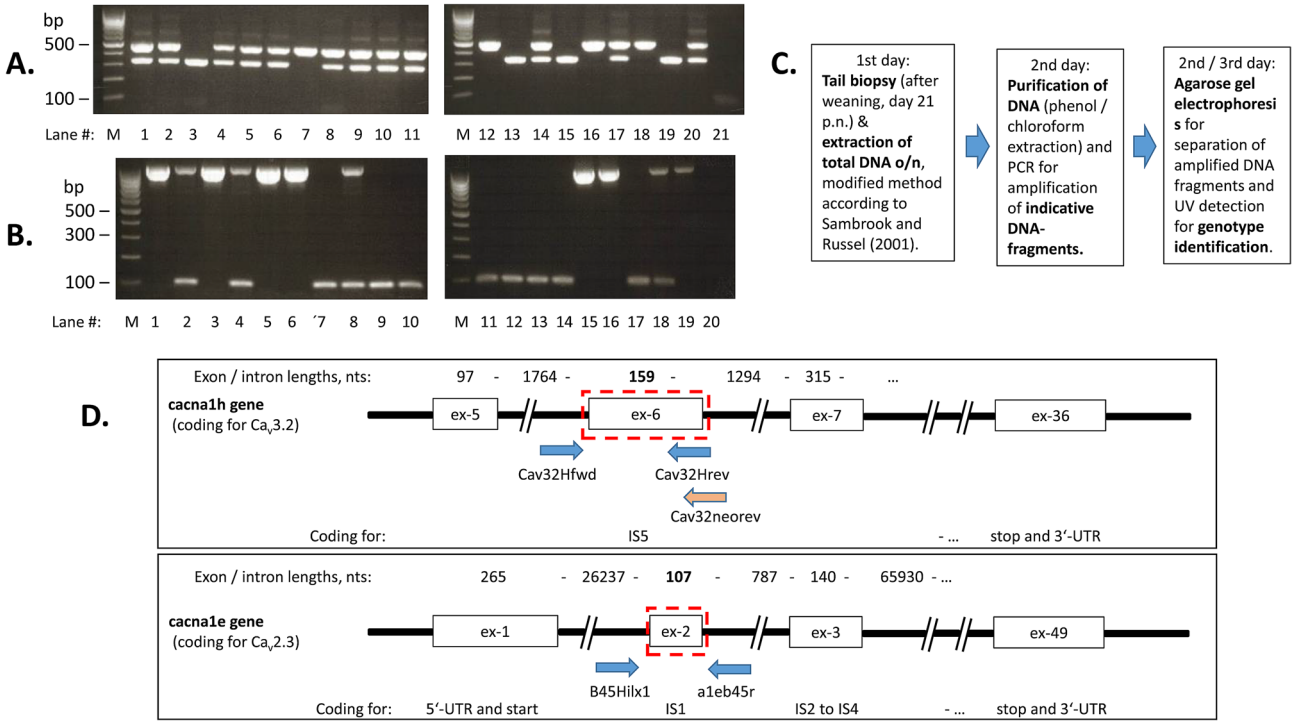

Figure 1. PCR-amplification of genotype specific DNA-fragments. Total DNA was isolated from tail biopsies of about 21 day old mice. M = size markers for double strand DNA, as indicated. Panel A and B are composed of two pictures, which are processed in parallel. (**A**) DNA-fragments indicative for $Ca_v3.2$-competent (480 bp) and $Ca_v3.2$-deficient mice (330 bp) from a typical screening experiment (lane 1 to lane 17). Double bands (480 and 330 bp) are indicative of heterozygous mice. Reference DNA from a WT control ($Ca_v3.2$-competent, lane 18), from a $Ca_v3.2$-KO mouse ($Ca_v3.2$-deficient, lane 19), and a known heterozygous mouse (lane 20) are introduced in each screening assay. Lane 21 shows the negative control, in which no tail-DNA was added. (**B**) DNA-fragments indicative for $Ca_v2.3$-competent (1056 bp) and $Ca_v2.3$-deficient mice (86 bp) from a typical screening experiment (lane 1 to lane 16). Double bands (1056 and 86 bp) are indicative of heterozygous mice. Reference DNA from a WT control ($Ca_v2.3$-competent, lane 17), from a $Ca_v2.3$-KO mouse ($Ca_v2.3$-deficient, lane 19), and a known heterozygous mouse (lane 18) are introduced in each screening assay. Lane 20 shows the negative control, in which no tail-DNA was added. (**C**) Schematic presentation the isolation of genomic DNA from tail biopsies and of genotyping by PCR. (**D**) Cartoon illustrating the gene structure, the position of primers used for genotyping and the deleted exons (dashed rectangular). *Upper panel* is showing the intron–exon structure for part of the cacna1h gene (total size 67,404 nts in humans, with 36 exons). Exon 6, encoding transmembrane segment S5 of domain I (IS5), was deleted by homologous recombination (further details: Chen CC et al., 2003), leading in the knockout allele to a novel sequence after ligation, so that only the novel reverse primer can hybridize complementarily. For the amplification of indicative cacna1h DNA-fragments from genomic DNA, the forward primer Cav32Hfwd (nts 4877–4898, Genbank ACH010580.2) and the reverse primer cav32Hrev (nts 5356–5335, GB AH010580.2) were used leading in the wild type mice to the expected fragments of 480 bp. For the $Ca_v3.2$-deficient mice the same forward but another reverse primer was used (Cav32neorev) unique for the deficient mice and leading to a fragment of 330 bp. *Lower panel* is showing the intron–exon structure for part of the cacna1e gene (total size 385,835 nts, in humans with 49 exons). Exon 2, encoding transmembrane segment S1 of domain I (IS1), was deleted by homologous recombination. Exon 2 represents nts 269 to 375 (GB L29346). In total, the sequence between the HindIII- and the NsiI-site was deleted (further details: Perverzev et al., 2002). For the amplification of indicative cacna1e DNA-fragments from genomic DNA, the forward primer B45Hilx1 (nts 87151–87173, GB AC101727.8) and the reverse primer a1eb45r (nts 88198–88177, GB AC101727.8) were used leading in the wild type mice to the expected fragments of 1056 bp and in the Ca_v23-deficient mice to a fragment of 86 bp.

by Western blotting using $Ca_v2.3$-selective antibodies. In heterozygous mice, the brain $Ca_v2.3$ protein level was about half of the amount detected in $Ca_v2.3$-competent mice[23,24].

$Ca_v2.3$ channels are inactivated by deleting exon 2 introducing an early stop codon. Exon 2 encoding the first transmembrane segment of the $Ca_v2.3$ Ca^{2+} channel was deleted by Cre-mediated recombination[23]. After inbreeding of heterozygous parents, the genotyping of the litter was performed postnatally by PCR on total DNA isolated from tail biopsies (Fig. 1B,C). The oligonucleotide primers were designed to detect reliably DNA fragments from all genotypes. The intensities of DNA fragments were sufficiently strong to identify wild type (6 mice plus 1 reference DNA), heterozygous (3 mice plus 1 reference DNA) and $Ca_v2.3$-deficient candidates (7

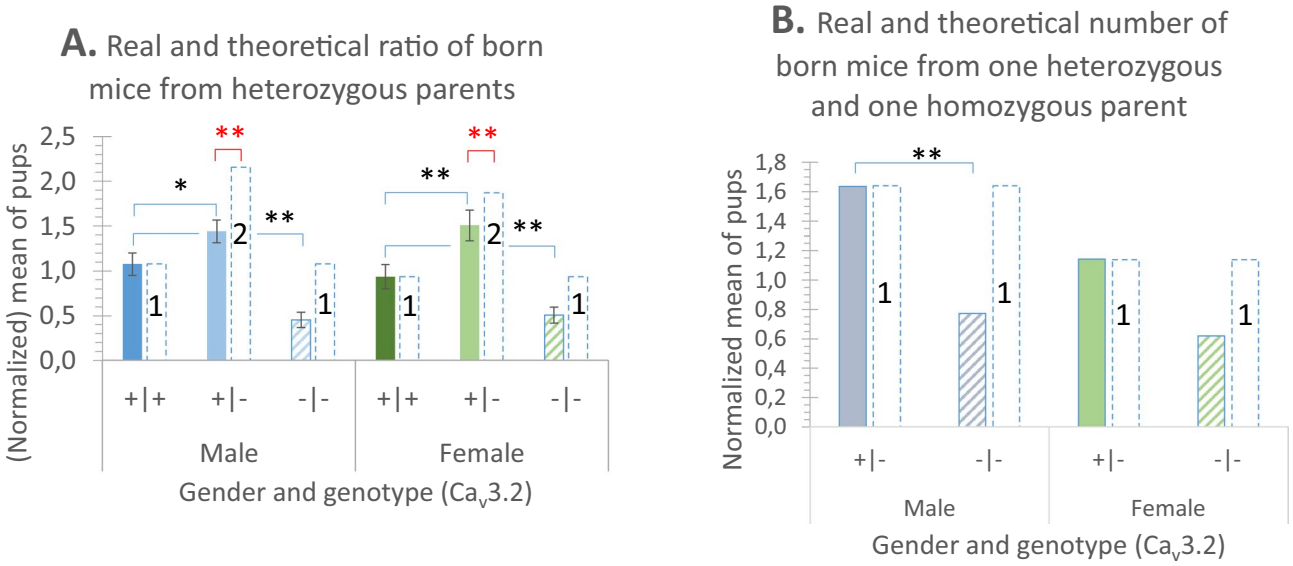

Figure 2. Genotype distribution profile of the offspring at the weaned stage by mating of $Ca_v3.2$ parents with various allele deficiencies. The bar columns terminated by dashed lines represent the theoretically predicted numbers when a Mendelian inheritance is assumed (related to the identified number of competent (+|+) pups). (**A**) Genotypes of the offspring from heterozygous $Ca_v3.2$(+|−) parents comparing the mean number of pups per mating. (**B**) Genotypes of the offspring from the mating of one heterozygous [$Ca_v3.2$(+|−)] and one homozygous [$Ca_v3.2$(−|−)] partner comparing the mean number of pups per mating.

candidates plus 1 reference DNA) (Fig. 1B). The negative control (no tail DNA included) did not contain DNA fragments of the references sizes (1056 bp for wt or 86 bp for KO).

Distribution of individual genotypes in the mouse lines for the $Ca_v2.3$ gene inactivation. During 63 breeding events from heterozygous parents, the mean litter size did not differ between male (3.6 ± 0.2) and female pups (3.3 ± 0.2) (Table 1). In total, 68 male $Ca_v3.2$(+|+) mice were born (Suppl.-Tab. 3. As null hypothesis and according to Gregor Mendel[20] one would expect 136 heterozygous and 68 homozygous male $Ca_v2.3$-deficient pups. But only 86 heterozygous mice were born. Different results were achieved for the females. During the same 63 breedings, in total 58 $Ca_v2.3$(+|+) female mice were born, 105 heterozygous and 44 $Ca_v2.3$-deficient pups were counted (Suppl.-Tab. 3). So far, only the number of heterozygous male mice was significantly different from the expected number (CHISQ $p < 0.005$) (Table 1). No deviation was observed for female pups (CHISQ $p > 0.1$) (Table 1 and Fig. 3), leading to the conclusion that in male mice the null hypothesis has to be rejected and that as an alternative hypothesis the inactivation of one allele of $Ca_v2.3$ must cause developmental problems, leading to a clear reduction of heterozygous male pups, which may only be compensated when both $Ca_v2.3$ alleles are missing.

Discussion

Our most important findings are related to deviations of genotype distributions from the expected normal Mendelian inheritance among weaned pups. For both Ca^{2+} channel types, the genotypes of the weaned offspring were significantly different from the expected Mendelian ratios.

To demonstrate that one may exclude a false genotyping, examples for the determination by PCR were included showing that indicative DNA-fragments could reliably be amplified. Further, an erroneous determination of sex can be excluded, because the sex determination was performed by an experienced coworker. If a continuous miss-determination of male heterozygous pups would have occurred, the number of heterozygote female pups must have been significantly elevated from the expected Mendelian ratio, which is not the case.

Another mistake, which could explain the "non-Mendelian ratios", would be if unintentionally the breeding pairs would not have been all heterozygous. We can exclude it, as all parents were re-genotyped when the breeding was started. Further, we checked the data for the $Ca_v3.2$-breedings and revealed in the 13 breeding lines (see Suppl.-Tab. 1) only a single breeding pair with no $Ca_v3.2$ null pups. For the $Ca_v2.3$-breeding data (see Suppl.-Tab. 3) we revealed in the 17 breeding lines only 2 of them, which did not have a Cav2.3 null pups.

So far, only for the ion conducting $Ca_v\alpha1$ subunit of the cardiac L-type Ca^{2+} channel a prenatal lethality is known[25]. No viable $Ca_v1.2$(−|−) mice were born, but the number of heterozygous pups was normal, corresponding to the expected Mendelian ratio. The developing $Ca_v1.2$-deficient pups died before day 14.5 postcoitum (p.c.) but up to day 12.5 p.c., the embryonic hearts contracted with identical frequency in wild type, heterozygous and homozygous $Ca_v1.2$ deficient mice. So far, it has remained unclear, which unidentified L-type like Ca^{2+} current may enable the normal prenatal beating between day 12.5 and 14.5 p.c. in $Ca_v1.2$-deficient mice[25,26].

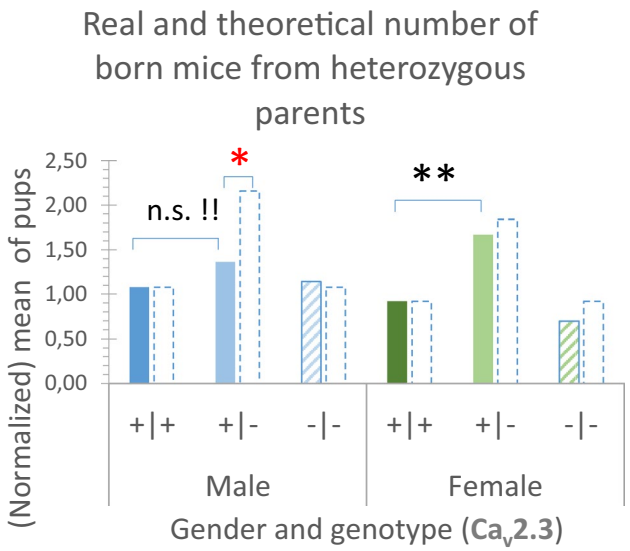

Figure 3. Genotype distribution profile of the offspring at the weaned stage by mating of heterozygous $Ca_v2.3(+|-)$ parents. The bar columns terminated by dashed lines represent the theoretically predicted numbers when a Mendelian inheritance is assumed (related to the identified number of competent (+|+) pups). Genotypes of the offspring comparing the mean number of pups per mating. Note that non-Mendelian inheritance is restricted to the male offspring only.

For the $Ca_v3.2$-deficient matings, a continuous reduction in the offspring number was observed for both sexes, when one or both alleles were inactivated in the pups. It is currently unknown and would be interesting to investigate, why the lack of the $Ca_v3.2$ allele causes prenatal lethality in some but not in all cases.

$Ca_v3.2$ belongs to the subfamily of low-voltage activated T-type Ca^{2+} channels. They are expressed in many developing tissues and involved in regulating cell proliferation, differentiation, growth and death[27]. Both, the development of T-type channel isotypes and the development of electrophysiologically defined T-type currents reveals higher levels during embryonic states compared to the postnatal development (see Fig. 1 in[27]. There is sufficient evidence for a high expression of T-type Ca^{2+} channels in embryonic tissues at the molecular level[28], which appears to be especially important for cardiac[29,30] and neuronal development[31,32].

Using information from the gnomAD data base, which quantifies the functional constraints for human genes, CACNA1H is not under significant functional constraint in the human population, though no individuals with homozygous loss of function alleles have been observed. Its o/e number with 0.38 (CI 0.28–0.5) is high, illustrating that the number of observed per expected (o/e) nucleotide variants found indicates a much higher functional constraint for CACNA1E, which is among the most constrained genes in the human genome with an o/e value of only 0.07 (CI 0.04–0.12).

While for the inherited mutations in humans, the functional constraints for the CACNA1E are much higher than for the CACNA1H gene, it does not seem to be the case for the investigated mouse models in the present study. The investigation of the role of the cacna1e gene in a neurotoxin Parkinson's mouse model revealed that the Cav2.3 knockout even reduced activity-associated nigral somatic Ca^{2+} signals and Ca^{2+}-dependent afterhyperpolarizations, leading to full protection from degeneration in vivo [2a].

On the other side, the o/e evaluation for the CACNA1E gene in the gnomAD data base fits well with the observation that de novo mutations in CACNA1E are critical. Recently, for $Ca_v2.3$ in 30 children de novo gain-of-function mutations were identified, which cause developmental and epileptic encephalopathy with contractures, macrocephaly and dyskinesias[33]). These disturbances in addition cause early death in the young patients.

The ion conducting subunit $Ca_v2.3$ forms the central pore of the pharmacoresistant R-type Ca^{2+} channels, which also exhibit higher expression levels during prenatal development than postnatally[34,35]. The sex specific effect of one allele loss in heterozygotes may relate to the function of $Ca_v2.3$ during acrosome formation[21,22]. Sperms lacking $Ca_v2.3$ show altered Ca^{2+} responses, a reduced acrosome reaction and a strong subfertility phenotype[36]. If the loss of one $Ca_v2.3$ allele affects the acrosome reaction substantially, the loss of both alleles in homozygous KOs could have triggered a corresponding compensation reaction, e.g. by upregulation of another voltage-gated Ca^{2+} channel.

Probably the sex-selective deviation from the Mendelian ratio may include sex-specific hormonal effects, similar as it was reported for effects of Zn^{2+} ions on glucose homeostasis[37].

In the literature, paradoxical inheritance with heterozygosity has been listed as one out of ten different non-Mendelian inheritance patterns[38]. Such rare cases of unusual segregation patterns are found in some specific diseases, as for example for glaucoma involving the K423E allele of *TIGR* (trabecular meshwork-inducible glucocorticoid response) gene, which is only seen in heterozygotes[39]. Obviously, the mutated proteins in homozygotes may still form functional response elements that interact with other proteins. Two additional examples

are reported in the same review, which are related to a defect in the ephrin-B1 gene and to the craniofrontonasal syndrome, for which even heterozygous females are more severely affected than hemizygous mutant males[40,41].

Conclusion and future perspectives

Our findings show that in depth investigations are needed to understand the prenatal developmental role of voltage-gated Ca^{2+} channels. For mutations of the human $Ca_v2.3$ R-type Ca^{2+} channel several gain-of-function mutations have been reported and they severely change the juvenile development during the mentioned developmental and epileptic encephalopathy[33]. A better understanding of this complex disease would help to find a better therapy for treating the children, which have a low life time expectancy.

Received: 10 September 2019; Accepted: 3 September 2020
Published online: 02 October 2020

References:

1. Southan, C. *et al.* The IUPHAR/BPS Guide to PHARMACOLOGY in 2016: towards curated quantitative interactions between 1300 protein targets and 6000 ligands. *Nucleic Acids Res.* **44**, D1054 (2016).
2. Berridge, M. J., Lipp, P. & Bootman, M. D. The versatility and universality of calcium signalling. *Nat Rev Mol. Cell. Biol.* **1**, 11–21 (2000).
3. Yunker, A. M. & McEnery, M. W. Low-voltage-activated ("T-Type") calcium channels in review. *J. Bioenerg. Biomembr.* **35**, 533–575 (2003).
4. Sochivko, D. *et al.* The a1E calcium channel subunit underlies R-type calcium current in hippocampal and cortical pyramidal neurons. *J. Physiol.* **542**, 699–710 (2002).
5. Dibue-Adjei, M. *et al.* Schneider, T Cav23 (R-Type) calcium channels are critical for mediating anticonvulsive and neuroprotective properties of lamotrigine in vivo. *Cell. Physiol. Biochem.* **44**, 935–947 (2017).
6. Leuranguer, V., Monteil, A., Bourinet, E., Dayanithi, G. & Nargeot, J. T-type calcium currents in rat cardiomyocytes during postnatal development: contribution to hormone secretion. *Am. J. Physiol. Heart Circ. Physiol.* **279**, H2540–H2548 (2000).
7. Neumaier, F. *et al.* Reciprocal modulation of Cav 2.3 voltage-gated calcium channels by copper(II) ions and kainic acid. *J. Neurochem.* **147**, 310–322 (2018).
8. Stewart, T. A. & Davis, F. M. An element for development: Calcium signaling in mammalian reproduction and development. *Biochim. Biophys. Acta Mol. Cell Res.* **1866**, 1230–1238 (2019).
9. Bourinet, E. *et al.* Silencing of the Cav3.2 T-type calcium channel gene in sensory neurons demonstrates its major role in nociception. *EMBO J.* **24**, 315–324 (2005).
10. Cohen, R. *et al.* Lipid modulation of calcium flux through CaV2.3 regulates acrosome exocytosis and fertilization. *Dev. Cell* **28**, 310–321 (2014).
11. Van Heyningen, V. & Yeyati, P. L. Mechanisms of non-Mendelian inheritance in genetic disease. *Hum. Mol. Genet.* **13**(2), R225-233 (2004).
12. Becker, A. J. *et al.* Transcriptional upregulation of Cav3.2 mediates epileptogenesis in the pilocarpine model of epilepsy. *J. Neurosci.* **28**, 13341–13353 (2008).
13. Striessnig, J. & Koschak, A. Exploring the function and pharmacotherapeutic potential of voltage-gated Ca^{2+} channels with gene knockout models. *Channels (Austin)* **2**, 233–251 (2008).
14. Helbig, K. L. *et al.* De novo pathogenic variants in CACNA1E cause developmental and epileptic encephalopathy with contractures, macrocephaly, and dyskinesias. *Am. J. Hum. Genet.* **103**, 666–678 (2018).
15. Morissette, J. *et al.* Homozygotes carrying an autosomal dominant TIGR mutation do not manifest glaucoma. *Nat. Genet.* **19**, 319–321 (1998).
16. Seisenberger, C. *et al.* Functional embryonic cardiomyocytes after disruption of the L-type alpha 1C (Cav1.2) calcium channel gene in the mouse. *J. Biol. Chem.* **275**, 39193–39199 (2000).
17. Carvill, G. L. Calcium channel dysfunction in epilepsy: gain of CACNA1E. *Epilepsy Curr.* https://doi.org/10.1177/1535759719845324 (2019).
18. Pereverzev, A. *et al.* Alternate splicing in the cytosolic II-III loop and the carboxy terminus of human E-type voltage-gated Ca^{2+} channels: electrophysiological characterization of isoforms. *Mol. Cell. Neurosci.* **21**, 352–365 (2002).
19. Galetin, T. *et al.* Pharmacoresistant CaV2.3 (E-/R-type) voltage-gated calcium channels influence heart rate dynamics and may contribute to cardiac impulse conduction. *Cell. Biochem. Funct.* **31**, 434–449 (2013).
20. Lory, P., Bidaud, I. & Chemin, J. T-type calcium channels in differentiation and proliferation. *Cell Calcium* **40**, 135–146 (2006).
21. Qu, Y. & Boutjdir, M. Gene expression of SERCA2a and L- and T-type Ca channels during human heart development. *Pediatr. Res.* **50**, 569–574 (2001).
22. Weiergraber, M., Henry, M., Radhakrishnan, K., Hescheler, J. & Schneider, T. Hippocampal seizure resistance and reduced neuronal excitotoxicity in mice lacking the Cav2.3 E/R-type voltage-gated calcium channel. *J. Neurophysiol.* **97**, 3660–3669 (2007).
23. Pereverzev, A. *et al.* Disturbances in glucose-tolerance, insulin-release, and stress-induced hyperglycemia upon disruption of the Ca(v)2.3 (alpha 1E) subunit of voltage-gated Ca(2+) channels. *Mol. Endocrinol.* **16**, 884–895 (2002).
24. Shcheglovitov, A. *et al.* Molecular and biophysical basis of glutamate and trace metal modulation of voltage-gated Ca(v)2.3 calcium channels. *J. Gen. Physiol.* **139**, 219–234 (2012).
25. Sakata, Y. *et al.* Cav2.3 (α1E) Ca2+ channel participates in the control of sperm function. *FEBS Lett.* **516**, 229–233 (2002).
26. Kang, H. W., Vitko, I., Lee, S. S., Perez-Reyes, E. & Lee, J. H. Structural determinants of the high affinity extracellular zinc binding site on Cav3.2 T-type calcium channels. *J. Biol. Chem.* **285**, 3271–3281 (2010).
27. Lipscombe, D. & Andrade, A. Calcium channel Ca_valpha1 splice isoforms: tissue specificity and drug action. *Curr. Mol. Pharmacol.* **8**, 22–31 (2015).
28. Wieland, I. *et al.* Mutations of the ephrin-B1 gene cause craniofrontonasal syndrome. *Am. J. Hum. Genet.* **74**, 1209–1215 (2004).
29. Drobinskaya, I., Neumaier, F., Pereverzev, A., Hescheler, J. & Schneider, T. Diethyldithiocarbamate-mediated zinc ion chelation reveals role of Cav23 channels in glucagon secretion. *Biochim. Biophys. Acta Mol. Cell. Res.* **1854**, 953–964 (2015).
30. Pereverzev, A. *et al.* Disturbances in glucose-tolerance, insulin-release and stress-induced hyperglycemia upon disruption of the Cav23 (α1E) subunit of voltage-gated Ca2+ channels. *Mol. Endocrinol.* **16**, 884–895 (2002).
31. Benkert, J. *et al.* Cav2.3 channels contribute to dopaminergic neuron loss in a model of Parkinson's disease. *Nat. Commun.* **10**, 5094. https://doi.org/10.1038/s41467-019-12834-x (2019).
32. Bijlenga, P. *et al.* T-type a1H Ca^{2+} channels are involved in Ca^{2+} signaling during terminal differentiation (fusion) of human myoblasts. *Proc. Natl. Acad. Sci. USA* **97**, 7627–7632 (2000).

33. Griffiths, AJFM, J.H., Suzuki, D.T., et al. An Introduction to Genetic Analysis. *National Library of Medicine, National Institutes of Health* (2000).
34. Ferron, L., Capuano, V., Deroubaix, E., Coulombe, A. & Renaud, J. F. Functional and molecular characterization of a T-type Ca^{2+} channel during fetal and postnatal rat heart development. *J Mol. Cell. Cardiol.* **34**, 533–546 (2002).
35. Klugbauer, N., Welling, A., Specht, V., Seisenberger, C. & Hofmann, F. L-type Ca^{2+} channels of the embryonic mouse heart. *Eur. J. Pharmacol.* **447**, 279–284 (2002).
36. Chen, C. C. *et al.* Abnormal coronary function in mice deficient in alpha1H T-type Ca^{2+} channels. *Science* **302**, 1416–1418 (2003).
37. Dolphin, A. C. Calcium channel diversity: multiple roles of calcium channel subunits. *Curr. Opin. Neurobiol.* **19**, 237–244 (2009).
38. Twigg, S. R. *et al.* Mutations of ephrin-B1 (EFNB1), a marker of tissue boundary formation, cause craniofrontonasal syndrome. *Proc. Natl. Acad. Sci. USA* **101**, 8652–8657 (2004).
39. Mendel, G. Versuche über Pflanzenhybride. *Verhandlungen des Naturforschenden Vereins in Brünn* **4**, 3–47 (1866).
40. Su, H. *et al.* Upregulation of a T-type Ca2+ channel causes a long-lasting modification of neuronal firing mode after status epilepticus. *J. Neurosci.* **22**, 3645–3655 (2002).
41. Wennemuth, G., Westenbroek, R. E., Xu, T., Hille, B. & Babcock, D. F. Cav2.2 and Cav 2,3 (N- and R-type) Ca2+ channels in depolarization-evoked entry of Ca2+ into mouse sperm. *J. Biol. Chem.* **275**, 21210–21217 (2000).
42. Zamponi, G. W. Targeting voltage-gated calcium channels in neurological and psychiatric diseases. *Nat. Rev. Drug Discov.* **15**, 19–34 (2016).

Acknowledgements

We would like to especially thank Priv.-Doz. Dr. E. Mahabir-Brenner and Dr. M. Guschlbauer, the leader of the local animal facilities, for their excellent support in our projects.

Author contributions

T.S. contributed to conception and design of the work, acquisition, analysis and interpretation of the data for the work, drafting the work and revising it critically for important intellectual content. S.A., R.C. and F.N. contributed to conception and design of the work and revising it critically for important intellectual content. J.H. contributed to conception and design of the work. All authors approved the final version of the manuscript and agree to be accountable for all aspects of the work in ensuring that questions related to the accuracy or integrity of any part of the work are appropriately investigated and resolved. All persons designated as authors qualify for authorship, and all those who qualify for authorship are listed.

Funding

Open Access funding enabled and organized by Projekt DEAL. This study was funded by a DFG / German Research Foundation Grant (Schn 387/21-1 and /21-2).

Competing interests

The authors declare no competing interests.

Additional information

Supplementary information is available for this paper at https://doi.org/10.1038/s41598-020-72912-9.

Correspondence and requests for materials should be addressed to T.S.

Reprints and permissions information is available at www.nature.com/reprints.

Publisher's note Springer Nature remains neutral with regard to jurisdictional claims in published maps and institutional affiliations.